Electronic Supplementary Material (ESI) for Chemical Communications

An electron-deficient metallocavitand with an unusual selectivity towards substituted benzene derivatives during co-crystallizations

Chang-Cang Huang*, Jian-Jun Liu, Yong Chen and Mei-Jin Lin*

College of chemistry and chemical engineering, Fuzhou University, P. R. China, 350108

E-mail: cchuang@fzu.edu.cn (Prof. C.-C. Huang)

meijin_lin@fzu.edu.cn (Prof. M.-J. Lin)

Table of Contents:

1. Experimental Details and Synthesis

Materials and Methods: benzoyl chloride (analytical reagent grade), potassium thiocyanate (analytical reagent grade), *p*-chlorophenoxyacetic acid (≥99%), and hydrazine hydrate (85%), *N*, *N*-dimethylacetamide (DMA, analytical reagent grade), dimethyl sulfoxide (DMSO, analytical reagent grade**)**, chloroform (analytical reagent grade), chlorobenzene (analytical reagent grade), bromobenzene (analytical reagent grade), iodobenzene (analytical reagent grade) and aniline (analytical reagent grade) were obtained from commercial suppliers. All chemicals and reagents were used as received unless otherwise stated. NMR spectra were recorded with a Bruker Avance 400 MHz NMR spectrometer. Chemical shifts are given in parts per million (ppm) and referred to TMS as internal standard. ^{1}H coupling constants *J* are given in Hertz (Hz). Flourier transformation infrared (FTIR) spectra were recorded from KBr discs on a Perkin–Elmer Spectrum 2000 FT-IR spectrometer. Powder X-ray diffraction (PXRD) patterns were recorded with a Rigaku MiniFlex-II X-Ray diffractometer with Cu Kα radiation (λ = 1.54178 Å) and mass spectra were recorded on a Thermo Fisher Scientific LCQ Fleet system. Fluorescence spectra were recorded on an Edinburgh Instrument FL/FS-920 fluorescent spectrometer at room temperature.

Synthesis:

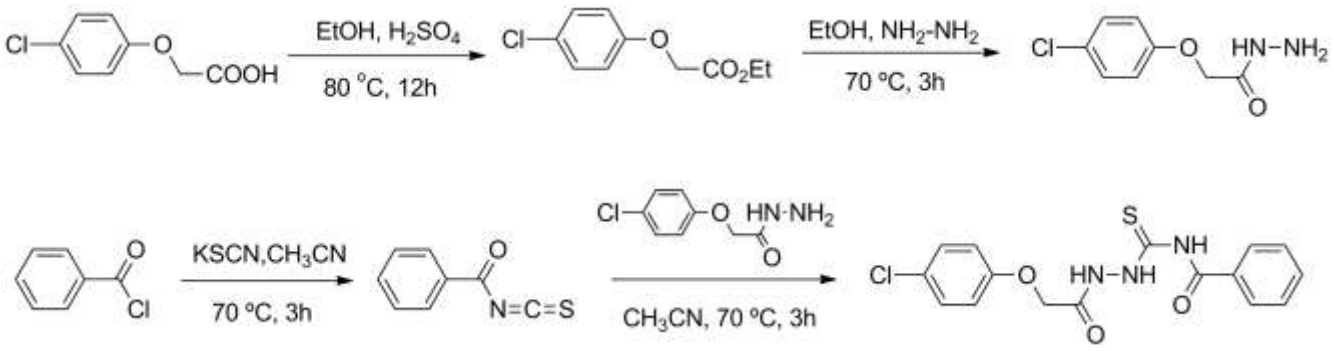

Scheme S1. Synthesis of building block **2**[S1]

Ethyl 2-(4-chlorophenoxy)acetate: Under the argon, 4 mL H_2SO_4 was slowly added to a solution of *p*-chlorophenoxyacetic acid (4.65 g, 0.025 mol) in ethanol (50 mL), then stirred at 80 °C for 12 hours. After being cooled to room temperature, the reaction mixture was neutralized by saturated sodium bicarbonate, and then the reaction mixture was extract by diethyl ether. Removal of the diethyl ether with rotary evaporator afford white ethyl 2-(4-chlorophenoxy)acetate, yield: 71%. ^{1}H NMR (400 MHz, DMSO-d_6, ppm): δ = 7.36-6.95 (m, 4H), 4.79 (s, 2H), 4.17 (q, J = 7.2 Hz, 2H), 1.21 (t, J = 7.2 Hz, 3H). ^{13}C NMR (100 MHz, DMSO-d_6, ppm): δ =169.0, 157.0, 129.7 (×2), 125.4, 116.8 (×2), 65.3, 61.1, 14.5.

2-(4-chlorophenoxy)acetohydrazide: Under the argon, a mixture of ethyl 2-(4-chlorophenoxy) acetate (3.80 g, 0.0175 mol) and hydrazine hydrate (85%) (3 mL, 0.05mol) were dissolved in 30 mL ethanol, and then stirred at 70 °C for 3 hours. After being cooled to room temperature, white crystalline 2-(4-chlorophenoxy)acetohydrazide was obtained by filtration, yield: 92%. ^{1}H NMR (400 MHz, DMSO-d_6, ppm): δ = 9.38 (s, 1H), 7.35-6.97 (m, 4H), 4.49 (s, 2H), 4.34 (s, 2H). ^{13}C NMR (100 MHz, DMSO-d_6, ppm): δ = 166.8, 157.1, 129.6 (×2), 125.3, 116.9 (×2), 66.9.

4-benzoyl-1-(2-(4-chlorophenoxy)acetyl)thiosemicarbazide: Under the argon, benzoyl chloride (1.41 g, 0.01 mol) was added to a solution of potassium thiocyanate (1.46 g, 0.015 mol) in acetonitrile (30 mL), and the mixture was stirred for 3 hours at 70 °C, and then filtered affording a yellow filtrate. 2-(4-chlorophenoxy)acetohydrazide (2.00 g, 0.01 mol) was added to the filtrate, and then stirred for further 3 hours at 70 °C to give a yellow precipitate, which was collected and rinsed with diethyl ether

(2×30 mL). Yield: 87%. ^{1}H NMR (400 MHz, DMSO-d_6, ppm): δ = 12.55(s, 1H), 11.80(s, 1H), 11.09(s, 1H), 7.98-7.04(m, 9H), 4.76(s, 2H). ^{13}C NMR (100 MHz, DMSO-d_6, ppm): δ = 178.7, 168.4, 165.3, 157.0, 133.6, 132.3, 129.7, 129.2, 128.9, 125.5, 117.1, 66.4. IR (KBr disk, υ cm^{-1}): 3334(m), 3277(m), 3038(w), 1673(s), 1601(m), 1569(m), 1528(s), 1472(s), 1439(s), 1357(m), 1245(s), 1065(m), 815(m), 677(m). MS (ESI-) *m/z* calculated for $C_{16}H_{14}ClN_3O_3S$: 363.04; found: 362.21.

Synthesis of complex 1: [Zn(acetylacetonate)$_2$(H_2O)] (56.3 mg, 0.2 mmol) and 4-benzoyl-1-(2-(4-chlorophenoxy)acetyl)thiosemicarbazide (72.6 mg, 0.2 mmol) were dissolved in DMA/$CHCl_3$ (1/1, v/v, 10mL), then the solution was stirred for 2 h at room temperature. The resulting colourless solution was filtered. After standing for several days, colourless plate crystals were obtained from the filtrate. Yield: 45% (based on **2**). ^{1}H NMR (400 MHz, DMSO-d_6, ppm): δ = 11.29 (s, 1H), 7.75-6.74(m, 9H), 4.47-4.19(m, 2H). IR (KBr disk, υ cm^{-1}): 3414 (w), 3096 (w), 3934(w), 1644(s), 1558(s), 1473(s), 1288(m), 1239(m), 1106(m), 1019(w), 790(m), 712(m), 647(m), 511(w).

Synthesis of complex 1⊃PhCl: complex **1** (200mg) was dissolved in DMA/DMSO/$CHCl_3$ (4/4/2, v/v/v, 10mL), and added to chlorobenzene (2mL, 20 mmol), then the solution was filtered. After staying for several days, colourless hexagonal crystals were obtained from the filtrate. Yield: 52%(based on complex **1**). Complex **1**⊃PhBr, **1**⊃PhI, **1**⊃$PhNH_2$ and **1**⊃$PhNO_2$ were also synthesized under similar reaction conditions and using the same molar ratios of reactants, except that bromobenzene, iodobenzene, aniline and nitrobenzene were used instead.

2. Single Crystal X-ray Diffraction Analyses

Suitable single crystals of building block **2,** complex **1**, **1**⊃PhCl, **1**⊃PhBr, **1**⊃PhI and **1**⊃$PhNO_2$ were mounted on glass fibers for the X-ray measurement. Diffraction data were collected on a Rigaku-AFC7 equipped with a Rigaku Saturn CCD area-detector system. The measurement was made by using graphic monochromatic Mo Kα radiation (λ= 0.71073 Å) at 113 K under a cold nitrogen stream. The frame data were integrated and absorption correction using a Rigaku *CrystalClear* program package. Data collection for **1**⊃$PhNH_2$ was performed on Rigaku-18 KW R-AXIS RAPID Weissenberg IP diffractometer equipped with graphite monochromated Mo-Kα radiation (λ = 0.71073 Å). All calculations were performed with the *SHELXTL-97* program package [S2], and structures were solved by direct methods and refined by full-matrix least-squares against F^2. All non-hydrogen atoms except for the disordered moieties were refined anisotropically, and hydrogen atoms of the organic ligands were generated theoretically onto the specific atoms and refined isotropically with fixed thermal factors. The diffraction data were treated by the "SQUEEZE" method as implemented in PLATON[S3] to remove diffuse electron density associated with these badly disordered solvent molecules. The included substituted benzene derivatives in the complex **1**, *i.e.* PhCl, PhBr, PhI and $PhNH_2$, were all disordered. For the 1⊃PhCl and 1⊃$PhNH_2$, the chlorobenzene and aniline molecules are equimolarly distributed at the both sides of the hourglass shaped inner cavities of complex 1 with the chlorine or amino groups situated towards the outside (Figure S2). However, for the 1⊃PhBr and 1⊃PhI, the distributions of the included substituted benzenes are more complex. Specifically, around 64% of the include PhBr (60% for PhI) molecules possessing a similar distribution pattern to that of the PhCl. Although the left molecules are also uniformly dispersed at the both sides of the hourglass shaped cavities, their aromatic ring groups are situated towards the outside (Figure S5). In addition, due to the poor diffraction data and disordered PhBr and PhI molecules in the crystal, so distance restraints and least-squares restraints were employed for PhBr and PhI. The host molecules in 1⊃PhCl, 1⊃PhBr, 1⊃PhI and 1⊃$PhNH_2$ possess three C_2 axes with 222 (D_2) symmetry. The inclusion assembled molecules in 1⊃PhCl, 1⊃PhBr, 1⊃PhI and 1⊃$PhNH_2$ possess pseudo-222 (D_2) symmetry imposed by crystallographic symmetry. Crystal data and refinement conditions are presented in below. Crystallographic data have been deposited with the Cambridge Crystallographic Data Center as

supplementary publication number CCDC-919044, 919054, 919055, 919056, 919064, 919334 and CCDC 935358 for building block 2, complex **1**, **1**⊃PhBr, **1**⊃PhI, **1**⊃$PhNH_2$, **1**⊃PhCl and **1**⊃$PhNO_2$, respectively. These data can be obtained free of charge from The Cambridge Crystallographic Data Centre *via* www.ccdc.cam.ac.uk/data_request/cif.

***Crystal data for* building block 2**: $C_{16}H_{14}ClN_3O_3S$, M_r = 363.81, colourless crystal, Monoclinic, Space group $P2_1/c$ (no. 14), a = 18.163(4) Å, b = 7.2623(15) Å, c = 13.383(3) Å, β = 110.81(3), V = 1650.0(6) $Å^3$, Z = 4, ρ_{calcd} = 1.465g·cm^{-3}, μ = 0.378 mm^{-1}, λ ($Mo_{K\alpha}$) =0.71073Å, F(000)=752, T = 293(2)K, *GooF* = 1.109, Final R indices: R_1 = 0.0576, wR_2 = 0.1197 for 3386 reflections [I >2σ(I)]; R_1 = 0.0664, wR_2 = 0.1243 for 3786 independent reflections (all data) [2θ ≤ 54.97°] and 217 parameters.

***Crystal data for* complex 1**: $Zn_8C_{188}H_{231}Cl_8N_{39}O_{39}S_8$, M_r=4724.16, colourless crystal, 0.42×0.23×0.20 mm^3, Triclinic, Space group P-1 (no.2), a=18.823(4) Å, b=19.042(4) Å, c=31.313(6) Å, α=96.46(3)°, β=102.02(3)°, γ=90.42(3)°, V=10902(4)$Å^3$, Z=2, ρ_{calcd} = 1.439 g·cm^{-3}, μ=1.117 mm^{-1}, λ ($Mo_{K\alpha}$)=0.71073Å, F(000)= 4896, T=113(2) K, *GooF* = 1.009, Final R indices: R_1 =0.0803, wR_2 =0.2066 for 29695 reflections [I >2σ(I)]; R_1 =0.1192, wR_2 =0.2294 for 48096 independent reflections (all data) [2θ ≤ 55.03°] and 1801 parameters.

***Crystal data for* 1⊃PhCl**: $Zn_8C_{186}H_{218}Cl_9N_{37}O_{37}S_8$, M_r =4662.46, colourless crystal, 0.37×0.28×0.23 mm^3, Orthorhombic, Space group Pban (no. 50), a=19.631 (4) Å, b=30.961(6) Å, c=18.383(4) Å, α=β=γ=90°, V=11173(4)$Å^3$, Z=2, ρ_{calcd}= 1.386 g·cm^{-3}, μ= 1.100 mm^{-1}, λ ($Mo_{K\alpha}$)=0.71073Å, F(000)= 4820, T=113(2) K, *GooF* =1.177. Final R indices: R_1 =0.1126, wR_2 =0.2790 for 11600 reflections [I >2σ (I)]; R_1 = 0.1205, wR_2 = 0.2846 for 12681 independent reflections (all data) [2θ ≤ 54.94°] and 483 parameters.

***Crystal data for* 1⊃PhBr**: $Zn_8C_{191}H_{236}BrCl_8N_{39}O_{39}S_8$, M_r = 4845.14, colourless crystal, 0.38×0.18×0.12 mm^3, Orthorhombic, Space group Pban (no. 50), a=19.493(4) Å, b=30.951(6) Å, c=18.295(4) Å, α=β=γ=90°, V=11038(4) $Å^3$, Z=2, ρ_{calcd} = 1.458 g·cm^{-3}, μ= 1.285 mm^{-1}, λ ($Mo_{K\alpha}$)=0.71073Å, F(000)= 5012, T=113(2) K, *GooF* = 1.133. Final R indices: R_1 =0.1085, wR_2

=0.2601 for 10203 reflections [$I > 2\sigma(I)$]; R_1 = 0.1341, wR_2 = 0.2772 for 12674 independent reflections (all data) [$2\theta \leq 55.07°$] and 489 parameters.

***Crystal data for* 1⊃PhI:** $Zn_8C_{210}H_{272}Cl_8IN_{43}O_{43}S_8$, M_r = 5276.65, colourless crystal, 0.28×0.18×0.14 mm^3, Orthorhombic, Space group Pban (no. 50), a=19.433(4) Å, b=31.567(6) Å, c=18.475(4) Å, α=β=γ=90°, V=11333(4)$Å^3$, Z=2, ρ_{calcd} = 1.546 $g \cdot cm^{-3}$, μ= 1.220 mm^{-1}, λ ($Mo_{K\alpha}$)=0.71073Å, F(000)= 5468, T=113(2) K, *GooF* = 1.254. Final R indices: R_1 =0.1553, wR_2 =0.3895 for 7310 reflections [$I > 2\sigma(I)$]; R_1 = 0.1993, wR_2 = 0.4219 for 12898 independent reflections (all data) [$2\theta \leq 54.97°$] and 488 parameters.

***Crystal data for* 1⊃PhNH$_2$:** $Zn_8C_{170}H_{103}Cl_8N_{34}O_{33}S_8$, M_r =4212.90, colourless crystal, 0.36×0.24×0.18 mm^3, Orthorhombic, Space group Pban (no. 50), a=19.839(4) Å, b=30.744(6) Å, c=18.652(4) Å, α=β=γ=90°, V=11376(4)$Å^3$, Z=2, ρ_{calcd} = 1.230 $g \cdot cm^{-3}$, μ= 1.060 mm^{-1}, λ ($Mo_{K\alpha}$)=0.71073Å, F(000)= 4258, T=293(2) K, *GooF* = 0.995. Final R indices: R_1 =0.0688, wR_2 =0.2089 for 7645 reflections [$I > 2\sigma(I)$]; R_1 = 0.1109, wR_2 = 0.2332 for 13032 independent reflections (all data) [$2\theta \leq 54.96°$] and 483 parameters.

***Crystal data for* 1⊃PhNO$_2$:** $Zn_8C_{192}H_{214.50}Cl_8N_{38.50}O_{41.50}S_8$, M_r = 4788.56, colourless crystal, 0.50×0.27×0.15 mm^3, Triclinic, Space group P-1 (no. 2), a=18.842(4) Å, b=18.915 (4) Å, c=31.455(6) Å, α=88.98(3)°, β=84.80(3)°, γ=89.60(3)°, V=11162(4)$Å^3$, Z=2, ρ_{calcd} = 1.425 $g \cdot cm^{-3}$, μ= 1.093 mm^{-1}, λ ($Mo_{K\alpha}$)=0.71073Å, F(000)= 4944, T=113(2) K, *GooF* =1.097. Final R indices: R_1 =0.0942, wR_2 =0.2327 for 36635 reflections [$I > 2\sigma(I)$]; R_1=0.1189, wR_2 = 0.2483 for 49239 independent reflections (all data) [$2\theta \leq 55.02°$] and 2100 parameters.

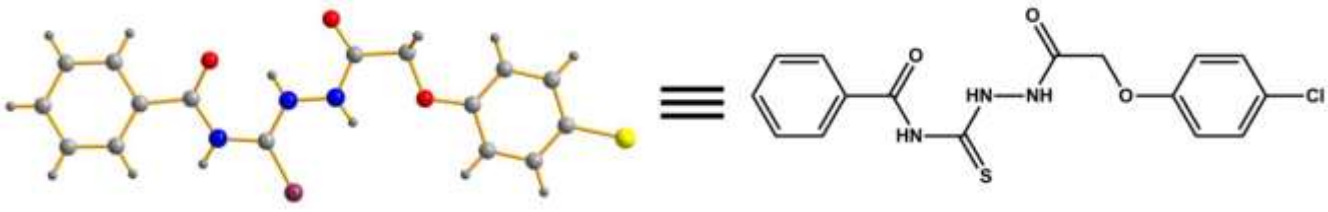

Figure S1. X-Ray single crystal structure of building block **2** (left) and chemical structure (right)

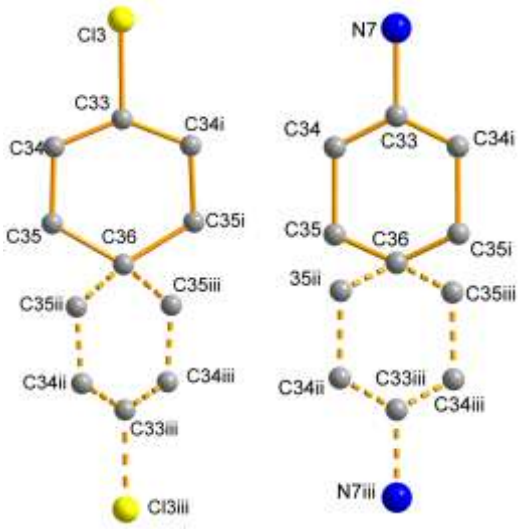

Figure S2. Disordered structures of chlorobenzene (left) and aniline (right) are shown with atomic labels. The atoms connected with stick form one of the ordered structures. [Symmetry code: (i) 1.5-x, y, 1-z; (ii) x, 0.5-y, 1-z; (iii) 1.5-x, 0.5-y, z]

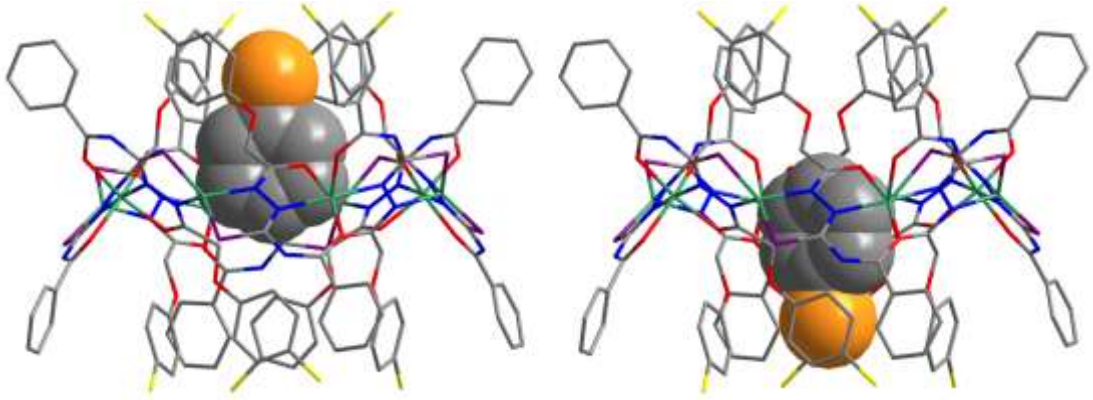

Figure S3. The two positions which chlorobenzene or aniline in the cavity. (green Zn, gray C, red O, blue N, purple S, yellow for Cl in *p*-chlorophenoxyl group, and orange for N in aniline or Cl in chlorobenzene)

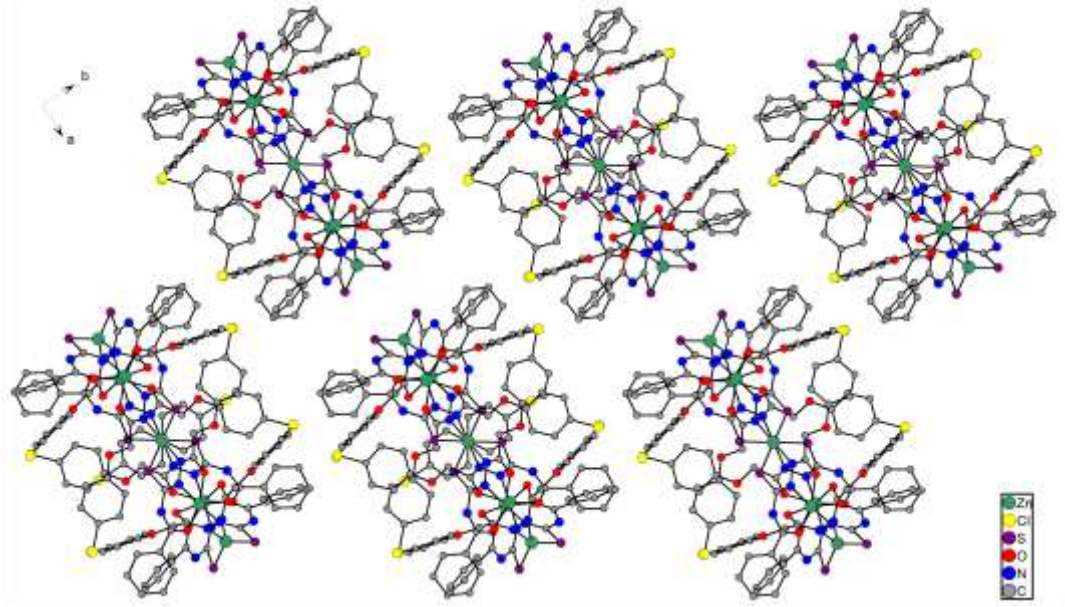

Figure S4. A view of the supramolecular framework of **1**⊃PhCl down *c* axis

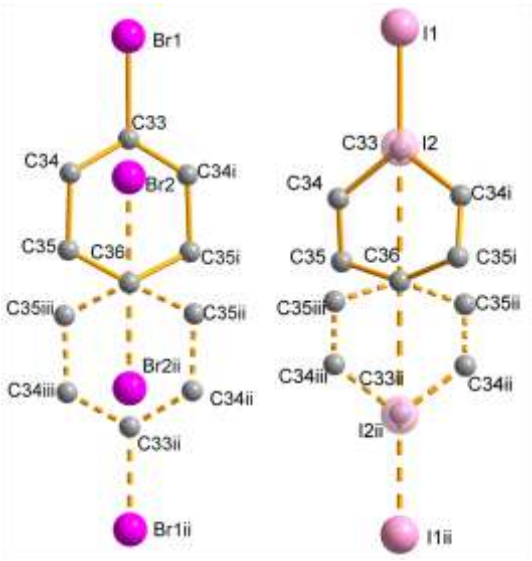

Figure S5. Disordered structures of bromobenzene (left) and iodobenzene (right) are shown with atomic labels. The atoms connected with stick form one of the ordered structures. [Symmetry code for bromobenzene: (i) 1.5-x, y, 2-z; (ii) 1.5-x, 0.5-y, z; (iii) x, 0.5-y, 2-z. Symmetry code for iodobenzene: (i) 0.5-x, y, 1-z; (ii) 0.5-x, 0.5-y, z; (iii) x, 0.5-y, 1-z]

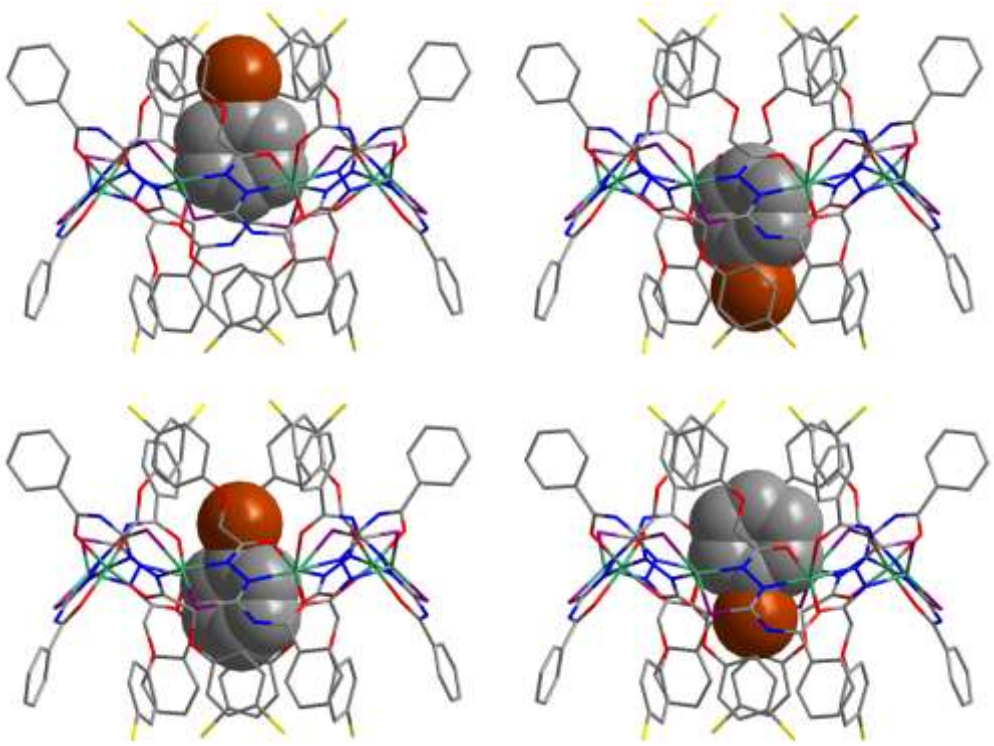

Figure S6. The four positions which bromobenzene or iodobenzene in the cavity. (green Zn, gray C, red O, blue N, purple S, yellow for Cl in *p*-chlorophenoxyl group, and brown for Br, or I of PhXs)

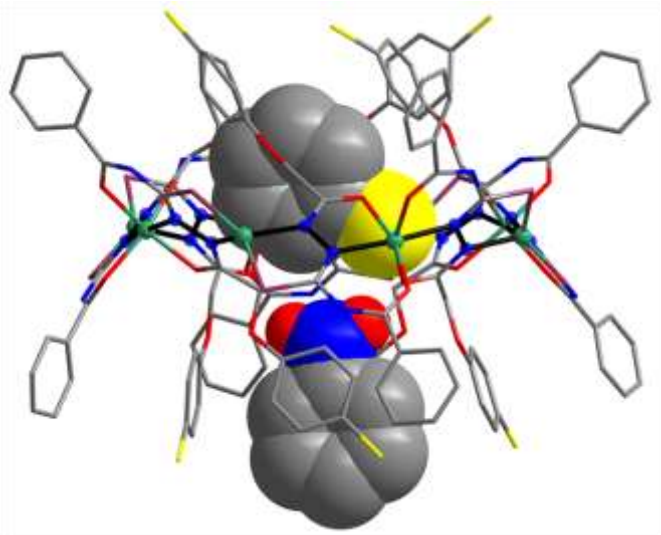

Figure S7. The side view of molecular structure of **1**⊃$PhNO_2$ in the crystal. (green Zn, gray C, red O, blue N, purple S, yellow Cl)

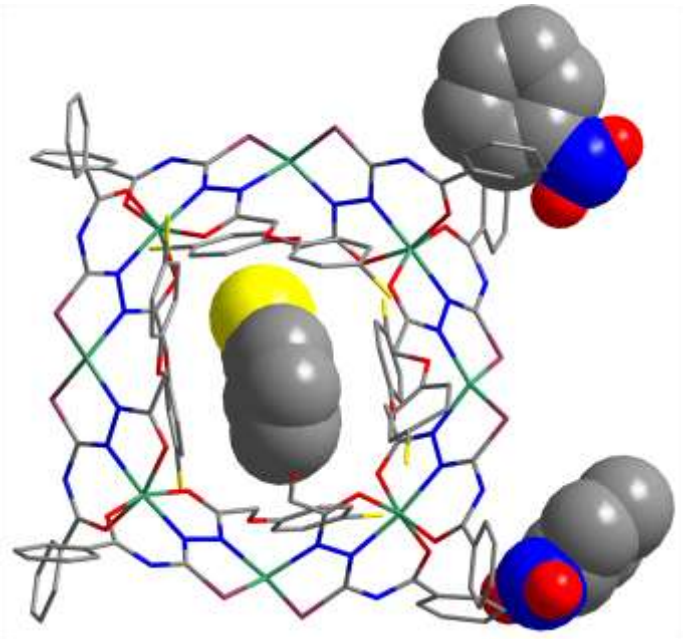

Figure S8. Two nitrobenzenes locate in the outside of cavity. (green Zn, gray C, red O, blue N, purple S, yellow Cl)

3. NMR Spectra

3.1 NMR spectra of the building block 2 4-benzoyl-1-(2-(4-chlorophenoxy)acetylthiosemicarbazide

The molecular structures of building block **2** was determined by single-crystal X-ray analysis and further confirmed by the ^{1}H and ^{13}C spectra. In the ^{1}H NMR spectrum of **2**, a sharp singlet at 4.76 ppm could be assigned to the methylene proton. Compared with this proton signal, two sharp singlets at 11.80 ppm and 11.09 ppm could be assigned to the proton of the hydrazide, and that at 12.55 ppm could be assigned to the proton of the amide. Moreover, those between 7.98-7.04 ppm (m, 9H) could be assigned to the proton of the benzene ring. These structural features are further supported by ^{13}C spectrum (Figure S10).

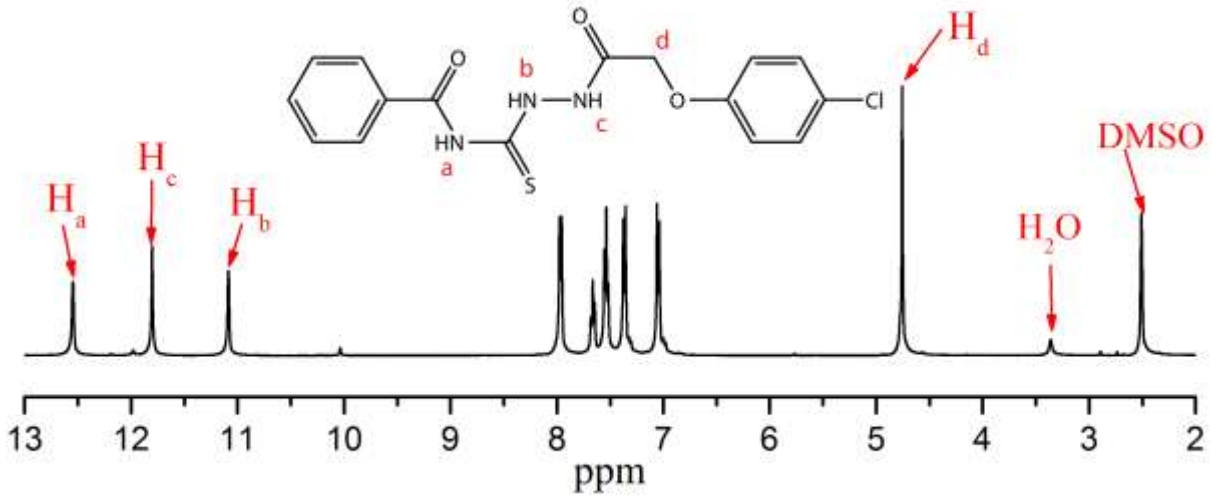

Figure S9. ^{1}H NMR spectrum of the 4-benzoyl-1-(2-(4-chlorophenoxy)acetyl)thiosemicarbazide in DMSO-d_6 (400 MHz, 293 K).

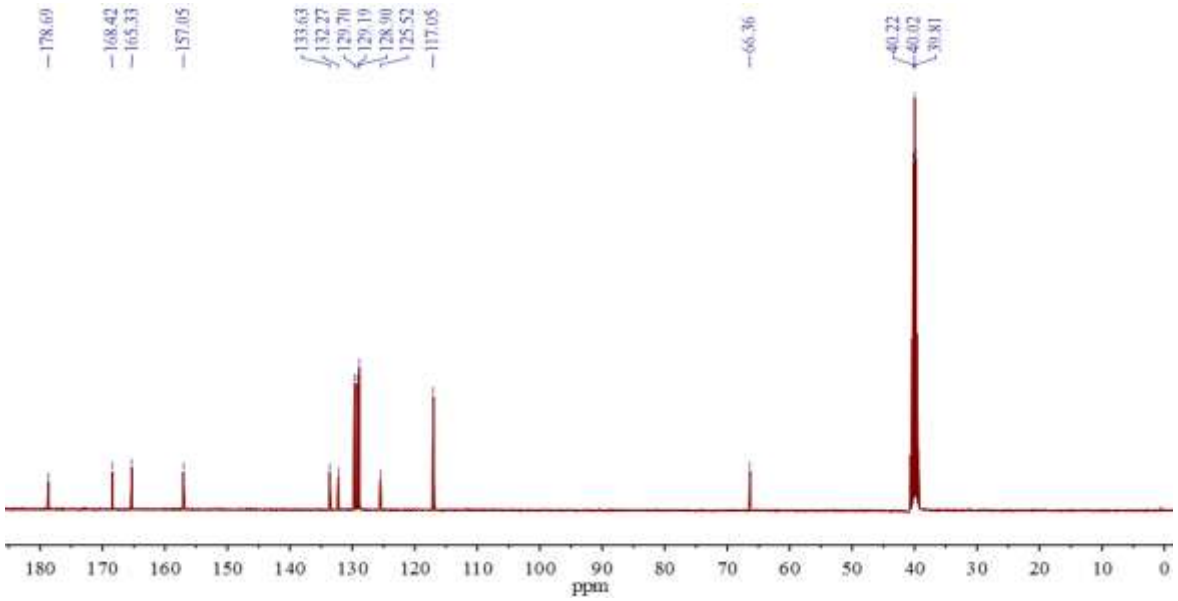

Figure S10. ^{13}C NMR spectrum of the 4-benzoyl-1-(2-(4-chlorophenoxy)acetyl)thiosemicarbazide in DMSO-d_6 (100 MHz, 293 K).

3.2 ^{1}H NMR spectra of complex 1

The chemical stability of complex **1** in solution is confirmed by its ^{1}H NMR spectrum in deuterated dimethyl sulfoxide. The proton signals at 11.29 (s, 1H) could be assigned to the proton of the not coordinated amide. Compared with the building block **2**, at 4.47 ppm (doublet, 1H) and 4.22 ppm (doublet, 1H) could be assigned to the methylene proton. Due to the eight methylene in the different chemical environments and large shielding effect of the ring, so there are two sets of peaks is moved to the high field.

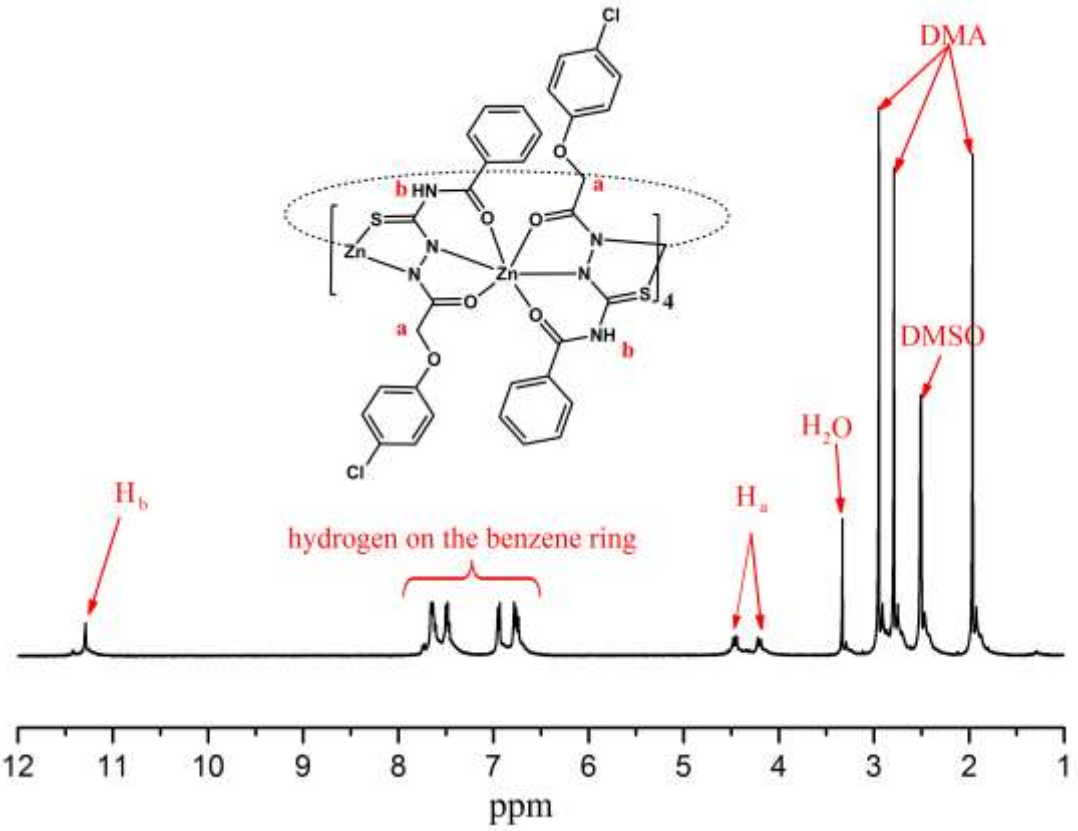

Figure S11. ^{1}H NMR spectrum of complex **1** in DMSO-d_6 (400 MHz, 293 K).

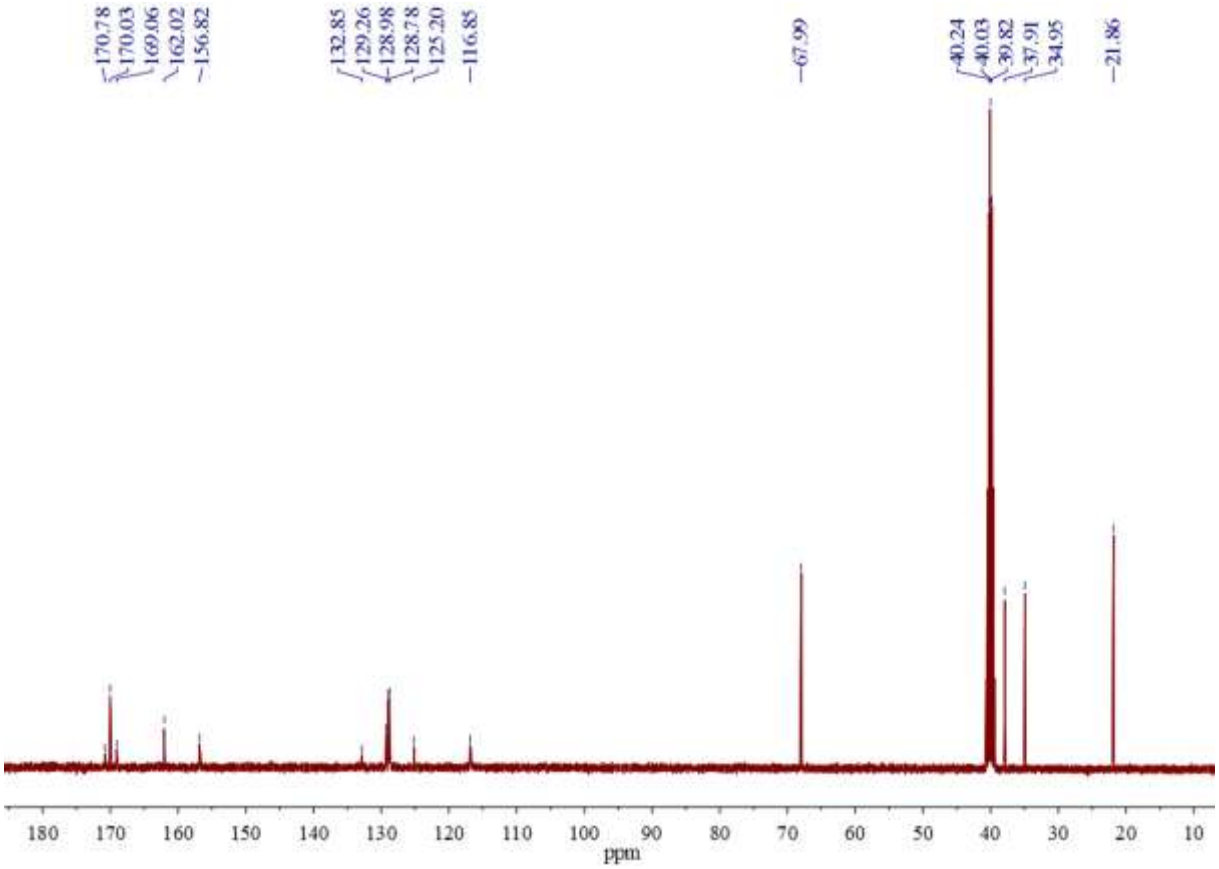

Figure S12. ^{13}C NMR spectrum of complex **1** in DMSO-d_6 (100 MHz, 293 K).

3.3 ^{19}F NMR spectra

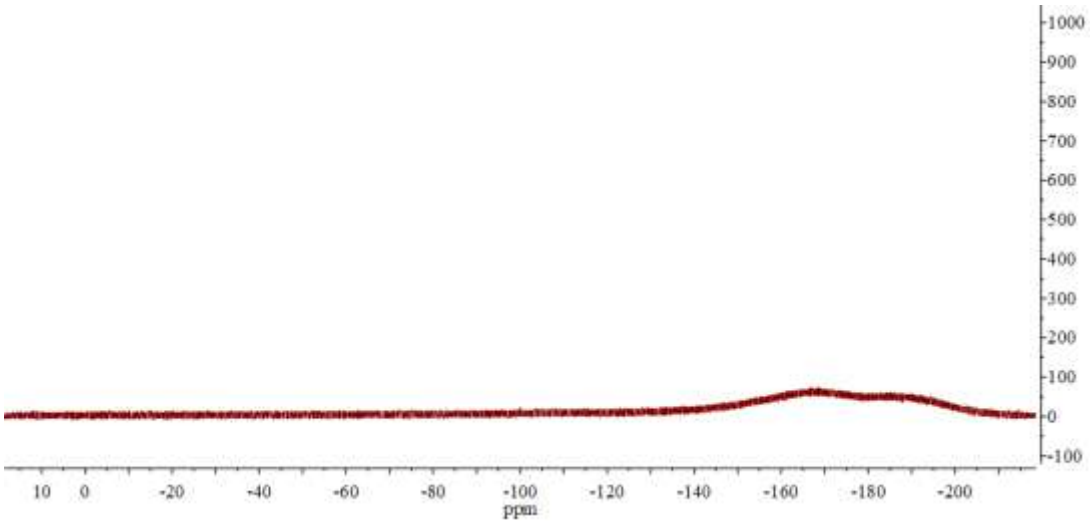

Figure S13. ^{19}F NMR spectrum of complex **1** of as-synthesized crystals obtained from PhF (376MHz, 293 K).

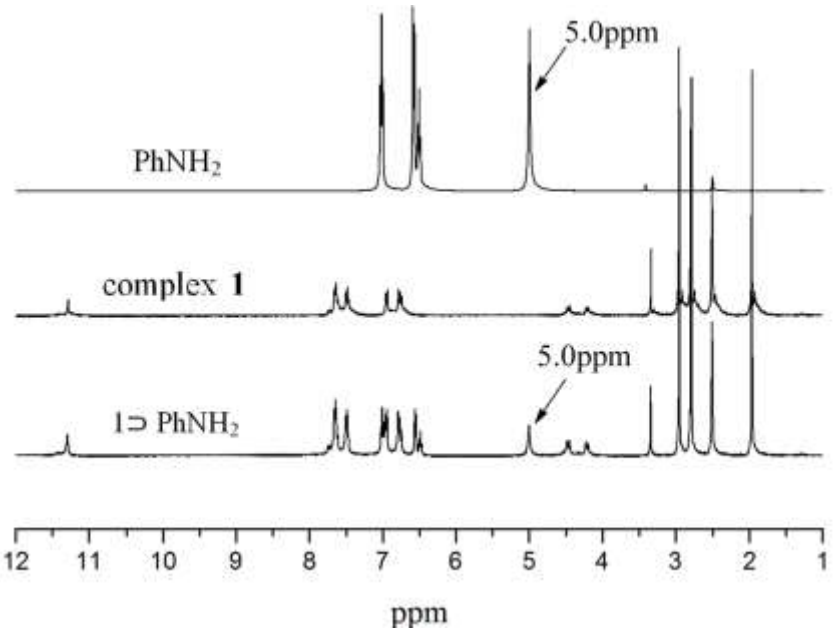

Figure S14. ^{1}H NMR spectrum (400 MHz, DMSO-d_6, 293K): top $PhNH_2$; middle complex **1**; bottom **1**⊃$PhNH_2$

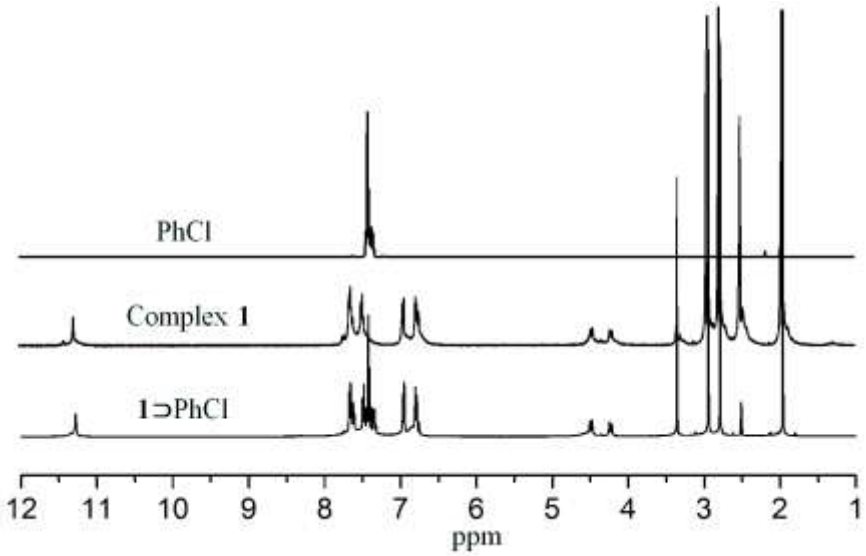

Figure S15. ^{1}H NMR spectrum (400 MHz, DMSO-d_6, 293K): top PhCl; middle complex **1**; bottom **1**⊃PhCl

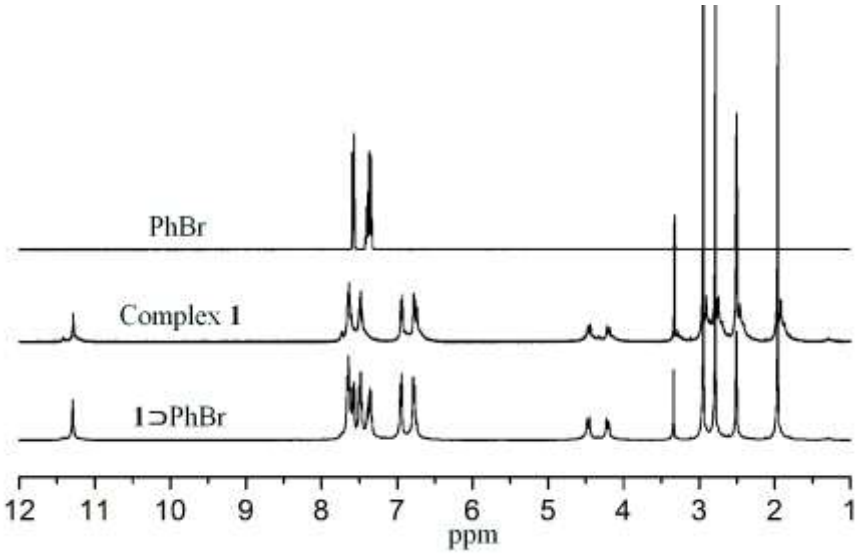

Figure S16. ^{1}H NMR spectrum (400 MHz, DMSO-d_6, 293K): top PhBr; middle complex **1**; bottom **1**⊃PhBr.

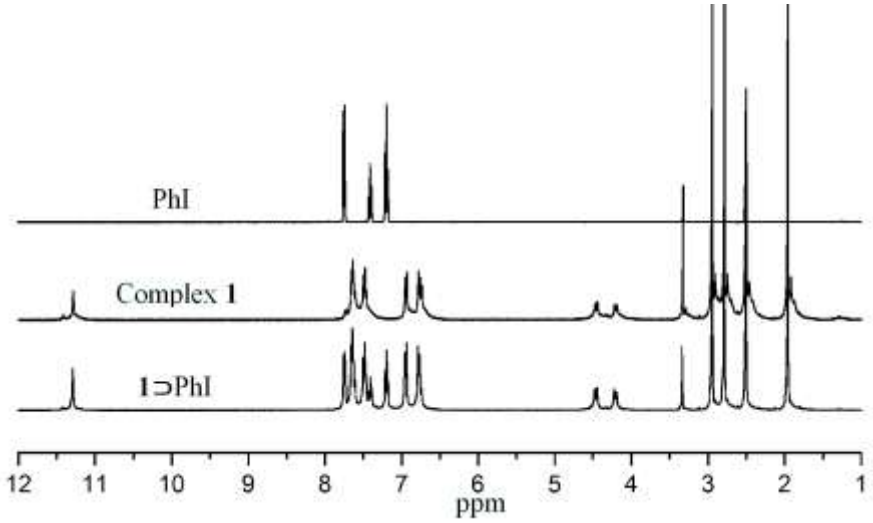

Figure S17. ^{1}H NMR spectrum (400 MHz, DMSO-d_6, 293K): top PhI; middle complex **1**; bottom **1**⊃PhI

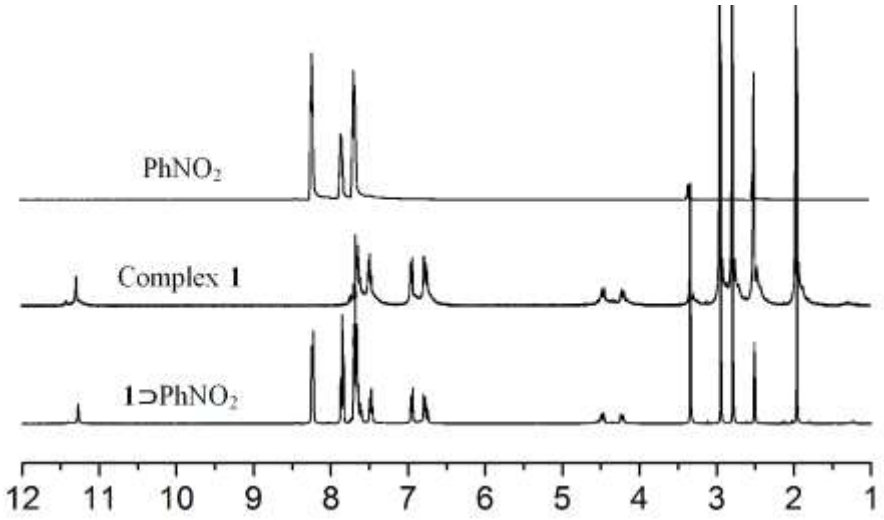

Figure S18. ^{1}H NMR spectrum (400 MHz, DMSO-d_6, 293K): top $PhNO_2$; middle complex **1**; bottom **1**⊃$PhNO_2$

4. Emission spectra

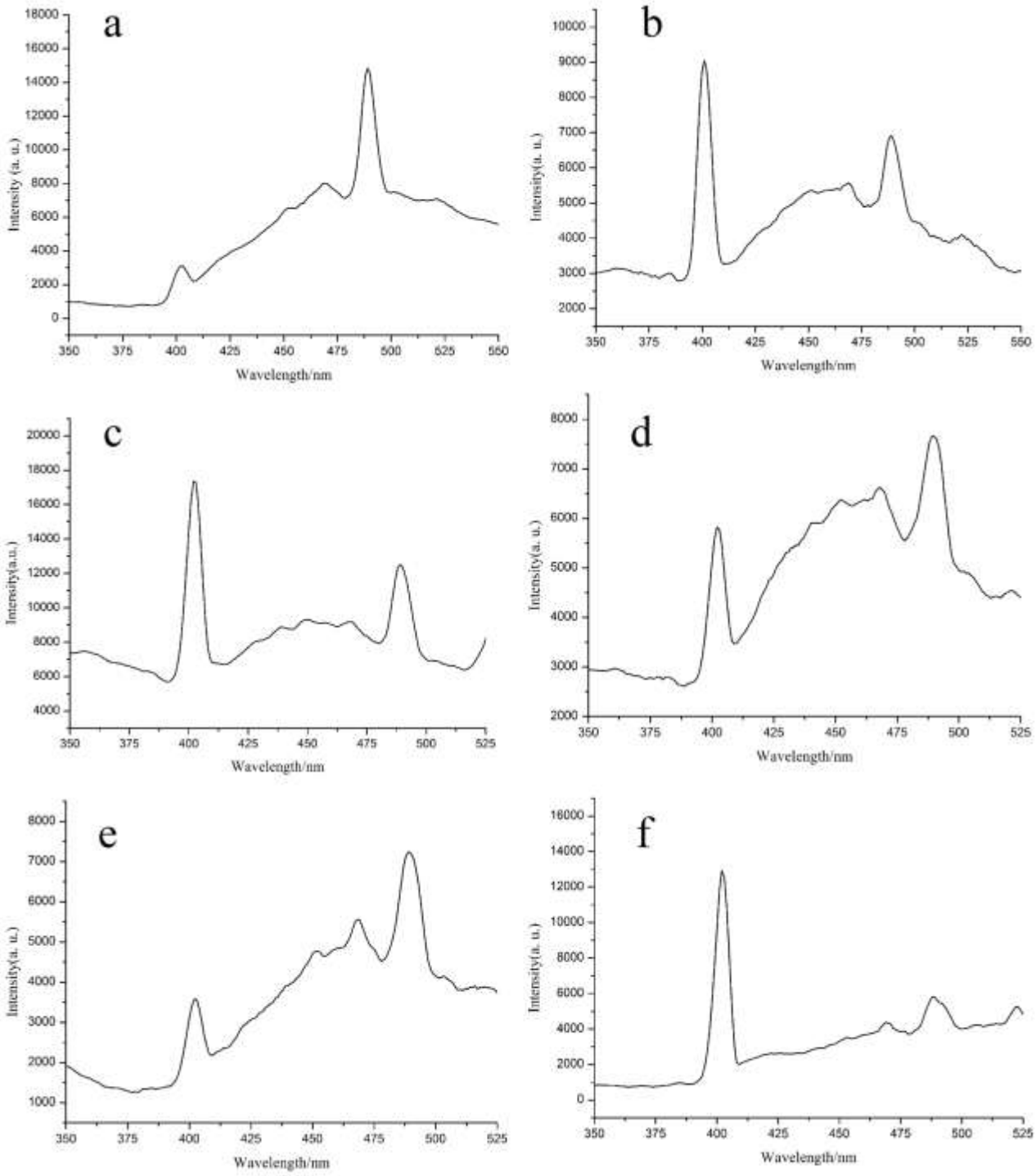

Figure S19. The luminescence spectra (excitation at 301nm). (a) complex **1**, (b) **1**⊃PhCl, (c) **1**⊃PhBr, (d) **1**⊃PhI, (e) **1**⊃$PhNH_2$, (f) **1**⊃$PhNO_2$

5. Thermogravimetric analyses

TGA measurements were performed on a TG-209 under a constant flow of nitrogen gas. Approximately 15 mg of sample was heated to 350 °C at a heating rate of 5 °C/min. The first weight loss (-27.7%) may be attributed to the loss of DMA molecules. The second weight loss until 300 °C is caused by the decomposition of complex **1**.

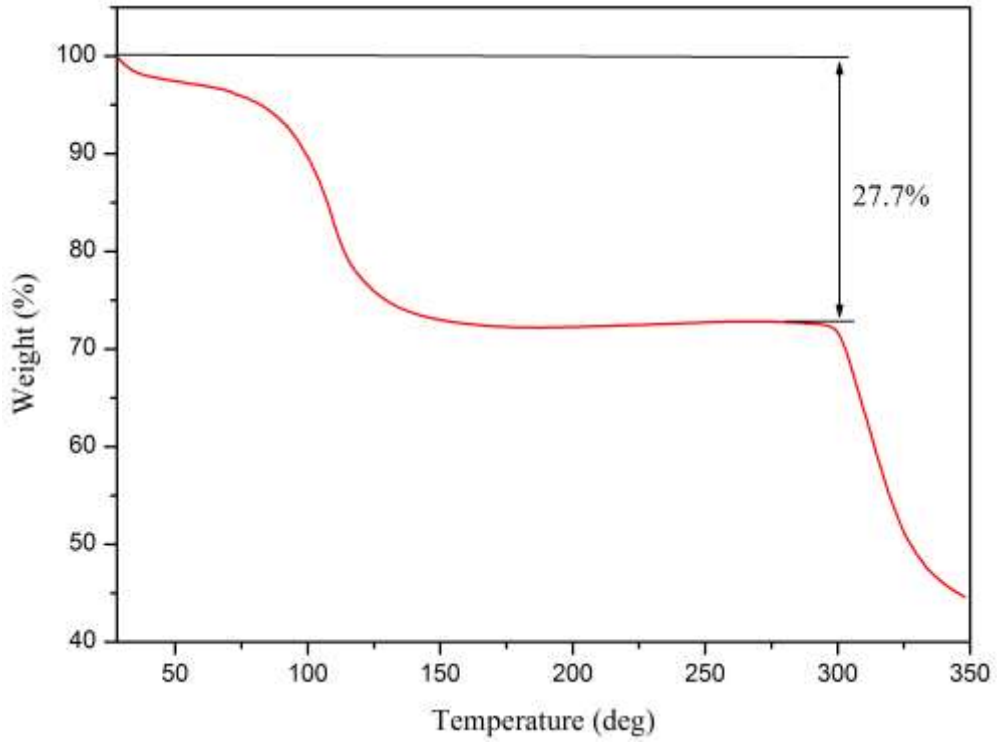

Figure S20. TGA thermograms of the complex **1**

6. X-ray Powder Diffraction

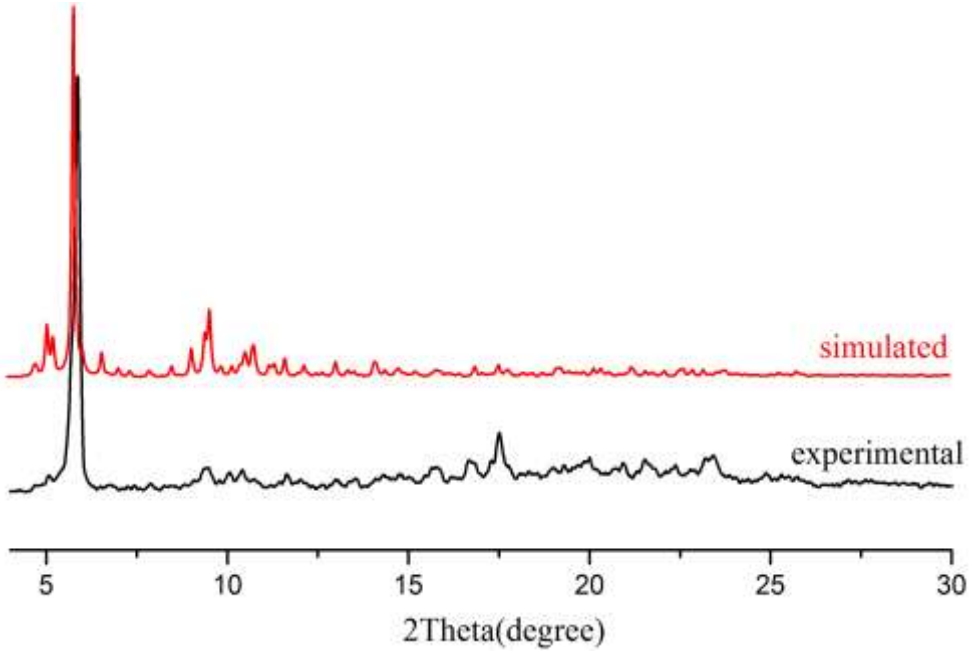

Figure S21. Experimental and simulated PXRD patterns for complex **1.**

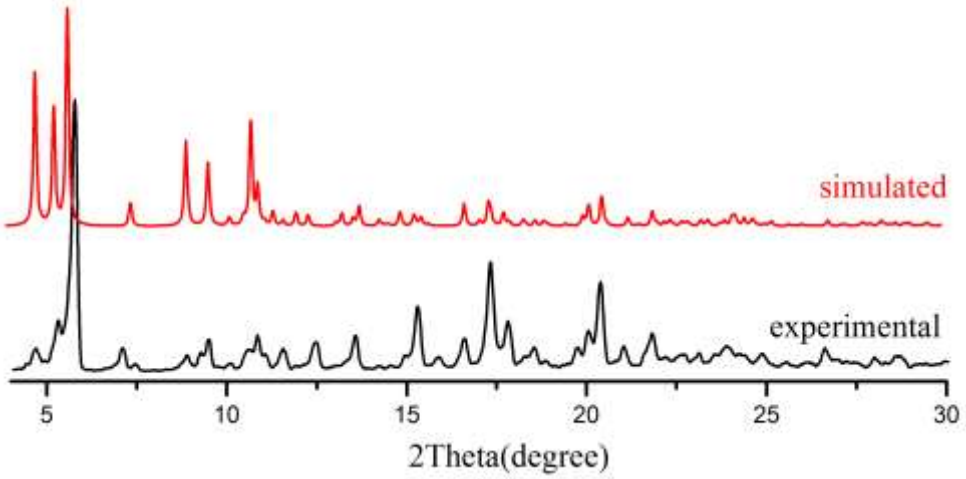

Figure S22. Experimental and simulated PXRD patterns for **1**⊃PhCl.

The different host-guest properties of complex **1** towards PhF and PhCl make it possible to be used as a microextractor for picking out PhCl from its PhF mixture. As expected, the dissolution of **1**, equimolar amounts of PhCl and PhF in a mixture solvent of DMA, DMSO and chloroform (4:4:2 in volume), followed by slow evaporation resulted in colourless hexagonal crystals of pure **1**⊃PhCl, which is confirmed by powder X-ray diffraction (PXRD) analysis (Figure S23a). To test the

sensitivity, an increase amount of PhF (3, 5 or 10 fold) was used in the recrystallization, which led to a mixture of complex **1** and **1**⊃PhCl in different ratios, respectively. PXRD revealed that the content of **1**⊃PhCl was decreasing with the increasing of the adding PhF ratio and almost no inclusion complex was detected when adding tenfold PhF. Similar conclusion can also be drawn by ^{1}H NMR spectroscopy as the proton signal intensities around 7.4 ppm of released PhCl, which is extracted from the same amount of as-synthesized crystals obtained from the different ratios of PhF/PhCl (1:1, 3:1, 5:1 or 10:1) by soaking in the deuterated acetonitrile for 6 hours, decreasing gradually with the increasing add PhF/PhCl ratios (Figure 23b). Instead, those of released DMA molecules between 1.5 to 3.0 ppm increase gradually. Anyhow, no PhF is observed in all the mixture crystals, which is verified by the ^{19}F NMR spectroscopy. The difficult formation of **1**⊃PhCl from the solution with a high adding PhF/PhCl ratio might be attributed to a kinetic factor, *i.e.* the formation of **1**⊃PhCl is a more kinetically unfavourable than that of complex **1** when adding more disturbed PhF molecules.

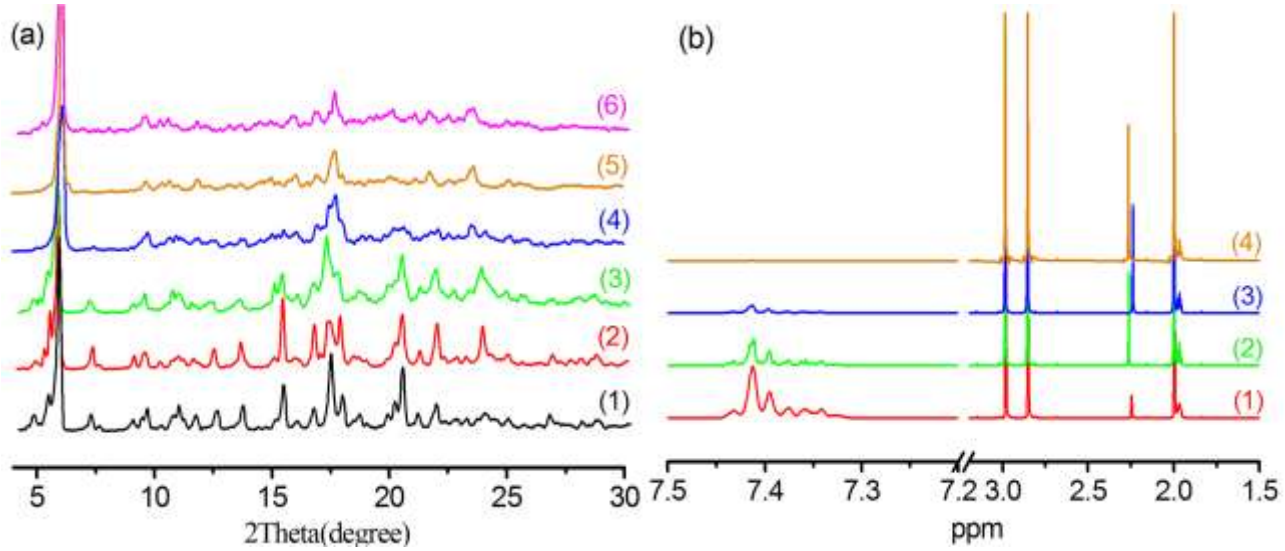

Figure S23: (a) the recorded PXRD patterns of as-synthesized crystals obtained from PhF/PhCl of different ratios ((2)1:1, (3) 3:1, (4) 5:1 and (5) 10:1) as well as those of pure 1 (6) and 1⊃PhCl (1) for comparison, and (b) the ^{1}H NMR spectra of PhCl that is extracted from the same amount of as-synthesized crystals obtained from PhF/ PhCl of different ratios ((1)1:1, (2) 3:1, (3) 5:1 and (4) 10:1) by soaking in deuterated acetonitrile for 6 hours at 288K.

7. Electrostatic Potential Calculation

Geometry optimizations of complex **1** was performed using the DFT hybrid functional B3LYP with the 6-21G* basis set as implemented in Gaussian03[S4]. The electron density map for the final geometry of the systems was calculated at B3LYP/6-31G** level. The electrostatic potential was to the full range at isovalue of 0.001 electrons/Bohr^3 for the electron density and was visualized by a brainbow color ramp continuously from red-orange-yellow-green-cyan-blue (electron rich to electron poor).

8. References

[S1] Wang, X. C.; Li, Z.; Da, Y. X.; Chen, J. C. *Synth. Commun*. **2000**, *30*, 3405-3412.

[S2] Sheldrick, G. *Acta Cryst.* **2008**, *A64*, 112-122.

[S3] Spek, A. L., Acta *Cryst.* **2009**, *D65*, 148-155.

[S4] M. J.Frisch, G. W. Trucks, H. B. Schlegel, G. E. Scuseria, M. A. Robb, J. R. Cheeseman, J. A. Montgomery Jr, T. Vreven, K. N. Kudin, J. C. Burant, J. M. Millam, S. S. Iyengar, J. Tomasi, V. Barone, B. Mennucci, M. Cossi, G. Scalmani, N. Rega, G. A. Petersson, H. Nakatsuji, M. Hada, M. Ehara, K. Toyota, R. Fukuda, J. Hasegawa, M. Ishida, T. Nakajima, Y. Honda, O. Kitao, H. Nakai, M. Klene, X. Li, J. E. Knox, H. P. Hratchian, J. B. Cross, V. Bakken, C. Adamo, J. Jaramillo, R. Gomperts, R. E. Stratmann, O. Yazyev, A. J. Austin, R. Cammi, C. Pomelli, J. W. Ochterski, P. Y. Ayala, K. Morokuma, G. A. Voth, P. Salvador, J. J. Dannenberg, V. G. Zakrzewski, S. Dapprich, A. D. Daniels, M. C. Strain, O. Farkas, D. K. Malick, A. D. Rabuck, K. Raghavachari, J. B. Foresman, J. V. Ortiz, Q. Cui, A. G. Baboul, S. Clifford, J. Cioslowski, B. B. Stefanov, G. Liu, A. Liashenko, P. Piskorz, I. Komaromi, R. L. Martin, D. J. Fox, T. Keith, M. A. Al-Laham, C. Y. Peng, A. Nanayakkara, M. Challacombe, P. M. W. Gill, B. Johnson, W. Chen, M. W. Wong, C. Gonzalez and J. A. Pople (2004) Gaussian 03, Gaussian Inc., Wallingford, CT.